Hindawi
International Journal of Polymer Science
Volume 2018, Article ID 8629894, 12 pages
https://doi.org/10.1155/2018/8629894

Research Article

Investigation of Drilling Parameters Using Grey Relational Analysis and Response Surface Methodology of Biaxial Glass Fibre Reinforced with Modified Epoxy Resin Composite

I Infanta Mary Priya[1] **and B. K. Vinayagam**[2]

[1]*Department of Mechanical Engineering, SRM Institute of Science and Technology, Chennai 603203, India*
[2]*Department of Mechatronics Engineering, SRM Institute of Science and Technology, Chennai 603203, India*

Correspondence should be addressed to I Infanta Mary Priya; infanta.i@ktr.srmuniv.ac.in

Received 18 December 2017; Revised 14 May 2018; Accepted 19 May 2018; Published 27 June 2018

Academic Editor: Michele Zappalorto

This research work attempts to study the most prominent factor of the drilling operations performed on different thicknesses of biaxial glass fibre reinforced with graphene platelet nanopowder and epoxy composite using three different drills. Damages are induced in the workpieces to analyse the effect of changed cutting parameters and different tool materials for varied thicknesses of the plates during the drilling process. The resultant drilled hole exhibited surface irregularities that are measured using SURFCOM 1400G. The circularity deviations of the holes are measured using a coordinate measuring machine. Image-processing technique is used to calculate the area of maximum diameter of the damaged zone. Using these data, delamination at entry and exit is calculated. Utilizing response surface methodology and grey relational analysis, the varied operations are carried out and analysed with different tool materials for common cutting parameters. It is found that the lesser thickness workpiece with selected HSS drill under high speed and low feed rate is the best variable option.

1. Introduction

Recent trends reveal that composite materials are extensively used in nearly all engineering fields from the automobile sector to the aircraft sector; these materials are favoured because of their inherent lightweight and achievable higher fibre aspect ratio. Rezende et al. [1] investigated the drill geometries on sandwich composites and observed that the tool selected and the speed were the most important factors which affected the thrust force, while the tool and feed rate played a major role in the burr height of the drilled hole. Though numerous research studies have been carried out in this area of machining process, very little literature documenting drilling operation data using different drill bits is available. Kumar et al. [2] studied the drilling process parameters such as feed, speed, and the drilled hole parameters such as delamination and surface roughness with three different materials of drill bits. For this study, the various drills used were HSS, carbide-tipped straight shank, and solid carbide eight-facet drill. The author concluded that the quality of the drilled holes was improved by using a solid carbide eight-facet drill. Babu et al. [3] studied the influence of drilling parameters on natural fibre-reinforced plastic with a cemented carbide drill, and the results were compared with GFRP composites. The analysis was carried out using the Taguchi technique as well as ANOVA. Thus, the authors were able to establish that feed rate and cutting velocity are the most influencing parameters with respect to delamination for various fibre-reinforced laminates. Various parts are manufactured using a FRP composite which requires machining operations such as drilling, milling, and grinding for the purpose of fastening, according to Grilo et al. [4]. Asiltürk and Neseli [5] developed a new method for the determination of optimal cutting parameters and a mathematical model for the evaluation of surface roughness. The system adopted for their study was noted to yield satisfactory results. Khashaba and El-Keran [6] studied the influence of speed and feed on thin glass fibre-reinforced woven composite. The parameters taken into consideration

for the analysis were cutting temperature, thrust force, torque, delamination factor, surface roughness, and bearing strength. The results showed that the delamination factor, torque, and thrust force increased with an increase in feed while the temperature induced increased with a decrease in feed. Debnath et al. [7] developed an innovative drill which was designed and made for the purpose of drilling on composite laminates. The authors found that the occurrence of damages from the developed forces was reduced when the operation was performed using the newly developed drill bit tool. Kulkarni et al. [8] investigated the drilling parameters of glass fibre reinforced with a carbon black vinyl ester composite. It was concluded that delamination was minimum with a tungsten carbide tool. From the scanning electron microscopic images, it was inferred that the delamination at the entry was minimum when compared to that at the exit side of the hole. In their study, Mohan et al. [9] performed drilling operation on a glass fibre-reinforced polymer composite and conducted delamination analysis. Their study predicted that peel-up delamination is influenced by specimen thickness and cutting speed. Similarly, push-down delamination is influenced by specimen thickness and feed rate. Confirmation tests were conducted which yielded 99% confidence level with the predicted results. Mudhukrishnan et al. [10] studied the influence of tool materials on the surface roughness of the drilled hole of glass fibre-reinforced polypropylene composites. Their study noted the drilled hole had a better surface finish when a solid carbide drill was used. Palanikumar and Davim [11] investigated the influence of tool wear parameters while machining GFRP composites. The results obtained from the experimental work and the analysis determined that the cutting speed is the major factor that influences the tool wear, with feed rate parameter a close second. Palanikumar [12] developed a model to determine delamination and surface roughness using surface roughness methodology. His ANOVA analysis showed that the results were within 95% confidence level. Sardinas et al. [13] performed a multiobjective optimization study on the process of drilling parameters such as delamination and material removal rate. The optimization process was carried out using genetic algorithms. The obtained results were represented graphically to determine their suitability for various processes. Sridharan et al. [14] studied the drilling process parameters on nanophased jute fibre-reinforced polymer composite. The authors adopted image-processing technique for the determination of the delamination factor. They also concluded that the addition of nanofiller material such as graphene enhanced the machinability of the composite material. Vankanti and Ganta [15] optimized the drilling process parameters using the Taguchi method. The authors found that feed rate is the most promising factor which influences thrust force, and cutting speed is the major factor affecting the torque. This methodology helped them not only to reduce delamination but also to meet drilled hole standard tolerance levels.

From various available literatures, it is found that no research work has been reported so far on the performance of drilling operation on a biaxial GFRP graphene platelet nanopowder composite. Usually, the delamination at entry and exit is measured by machine vision technique. In this research work, two different methods are used for analysing the optimal drilling parameters. One method is response surface methodology and the other is grey relational analysis. It is found that by using these two methods, the optimal results obtained are the same. The most suitable tool for drilling a nano-based GFRP composite is the HSS drill bit, and it yields minimum delamination at the entry and exit of the drilled hole with the lesser thickness (2 mm) specimen under high speed and low feed rate operations. The hole drilled using the HSS tool also gives minimum surface roughness and maximum circularity when compared to other titanium-coated HSS and carbide tip drill tools.

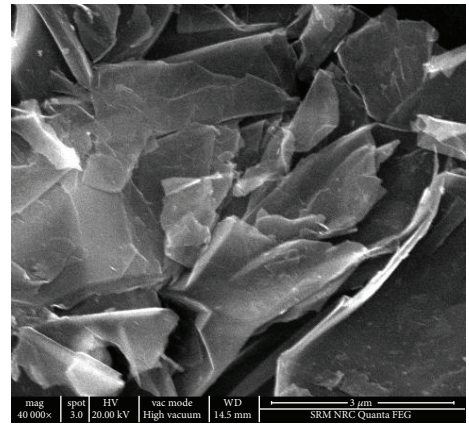

Figure 1: SEM image of the graphene platelet nanopowder.

2. Materials Used for the Study

This work involves the study of drilling operation on a biaxial glass fibre-reinforced polymer composite material. The material used for this study is a biaxial glass cloth of 600 gsm aerial density, purchased from Easy Composites, UK, and the laminates are prepared using hand lay-up method. Initially, bisphenol-A epoxy resin of grade LY556 is stirred thoroughly using a mechanical stirrer for 4 hrs, and then 0.1% weight of graphene platelet nanopowder is blended into the continuously stirred epoxy resin for another 4 hrs. Immediately after blending, 1 part of araldite hardener of grade HY951 is added to the blended resin mixture and infused to make the laminates. SEM image of the graphene platelet nanopowder is shown in Figure 1 to a magnification of 40,000x with particle size of 3 μm. Two sets of laminates are made to a thickness of 2 mm and 3 mm using the hand lay-up method. Then, the laminates are compressed in a compression moulding machine at 20 bar pressure and at a temperature of 80°C for 4 hrs after which it is allowed to cure for 24 hrs. Thus, the laminates are prepared and made ready for quality tests. They are then cut into test piece sizes of 100×100 mm. The drilling operation is performed in the vertical machining centre using three different drills (HSS drill, titanium-coated HSS, and carbide tip drill) of 10 mm diameter. The experimental set-up with the HSS drill bit is shown in Figure 2, and the various drills used are shown in Figure 3. Table 1

Figure 2: Experimental set-up.

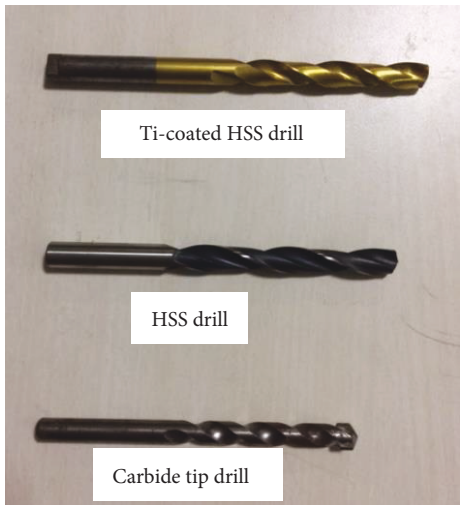

Figure 3: Types of drill bits used for the drilling operation.

gives the specification details of the different material drills used for the present study.

Figures 4(a) and 4(b) above show the drilled samples at the entry and exit sides, respectively, of the holes. Figure 4(a) shows that there is a minimum delamination at the entry side for all the three different drills while Figure 4(b) shows that there is maximum delamination with the titanium-coated HSS drill when compared to both the HSS drill and carbide tip drill at the exit side of the hole.

3. Experimental Work

3.1. Delamination Measurement. Delamination during drilling operation occurs in two ways—peel up and push out.

Table 1: Drilling details.

Parameter	Description
Drill tool materials	HSS drill, titanium-coated HSS drill, carbide tip drill
Diameter	10 mm
Geometry and type	Twist drill and straight shank
Point angle	118°
Machining condition	Dry
Feed rates (m/min)	50, 100, 150
Speed (rpm)	800, 1000, 1200

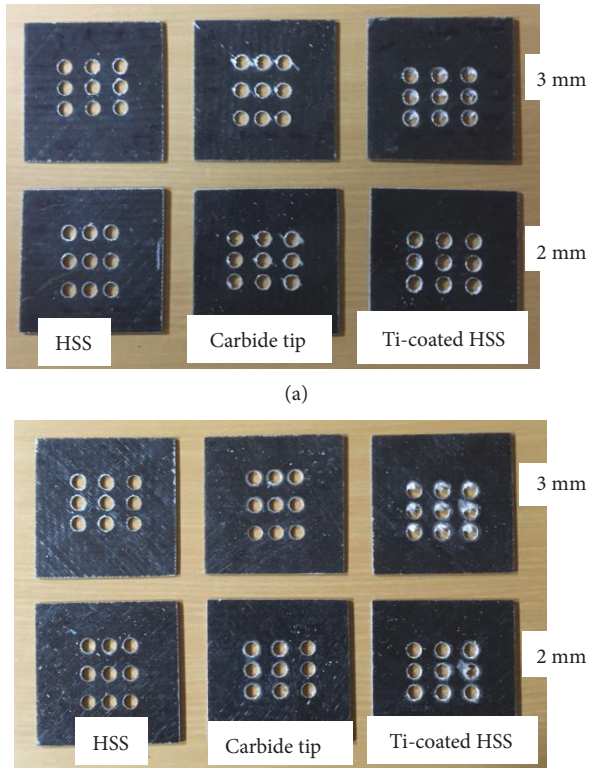

Figure 4: (a) Drilled samples at the entry side. (b) Drilled samples at the exit side.

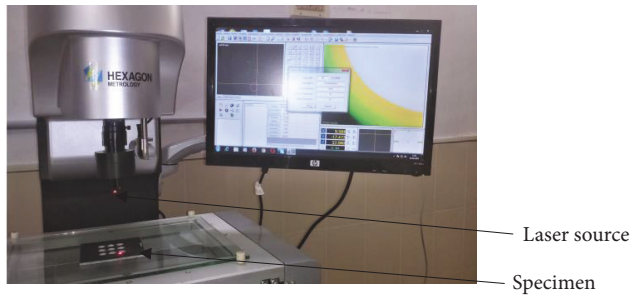

Figure 5: Delamination measurement at the entry and exit.

During drilling operation, the drill tool grazes the workpiece as the tool touches the specimen. The chips formed during the drilling operation gets pulled out in spiral form along

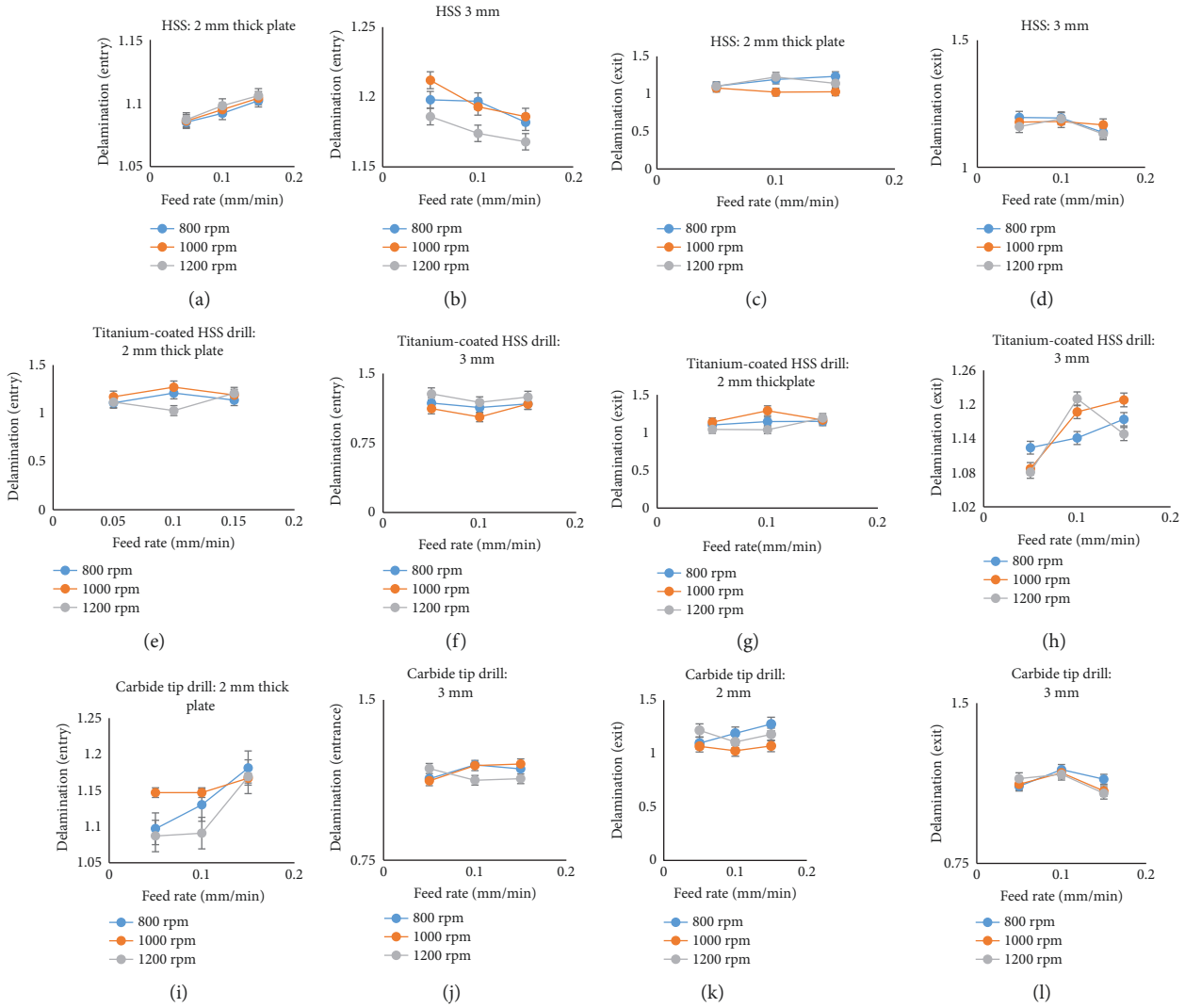

Figure 6: Delamination at entrance and exit under three different drills. (a, c, e, g, i, k) Delamination at the entry and exit of a 2 mm thickness specimen. (b, d, f, h, j, l) Delamination at the entry and exit of a 3 mm thickness specimen. (a, b) Delamination at the entrance. (c, d) Delamination at the exit. (e, f) Delamination at the entrance. (g, h) Delamination at the exit. (i, j) Delamination at the entrance. (k, l) Delamination at the exit.

Figure 7: Measurement of surface roughness.

the flute. As a consequence, the top surface of the laminate peels up first causing the defect called peel-up delamination. As the drilling operation progresses, the drill bit exerts compressive force which tends to bend the uncut plies elastically at the exit. At the same time, as the drill approaches the end of the process, there is a reduction in pressure due to less number of uncut plies which tends to reduce the resistance of bending in plies. Cracks develop adjacent to the hole because of increase in bending stress and weakening of interlaminar strength in the plies. As it drills down, the cracks get propagated further due to decrease in flexural rigidity. Due to this phenomenon, the bonding of interlamina fails which results in push-out delamination. But in the case of the carbide tip drill, there are two facets present for cutting, and there is a surface contact by means of the chisel edge of the tool. Since the concentration of the load at the surface contact increases, it causes irregularities around the drilled hole. The increased concentration of the load at the surface contact causes more irregularities in the area around the drilled hole.

Delamination is measured using machine vision Optiv Lite OLM 3020 model with a colour CCD camera of 1/3″ high-resolution capacity attached with VMS 3.1 software.

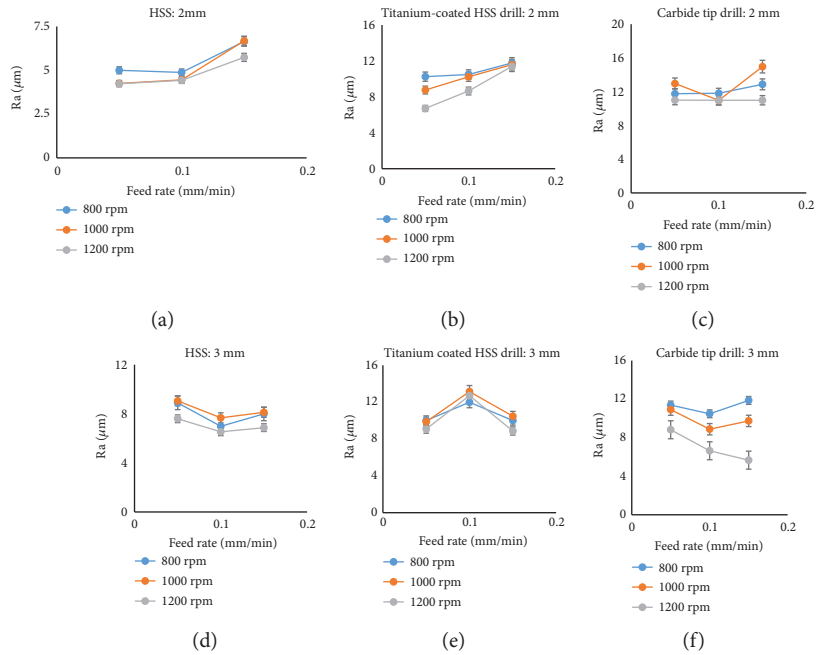

Figure 8: Surface roughness for 2 and 3 mm thickness specimens under three different drills. (a–c) Surface roughness of the 2 mm sample with (a) HSS drill, (b) titanium-coated HSS drill, and (c) carbide tip drill. (d–f) Surface roughness of the 3 mm sample with (d) HSS drill, (e) titanium-coated HSS drill, and (f) carbide tip drill.

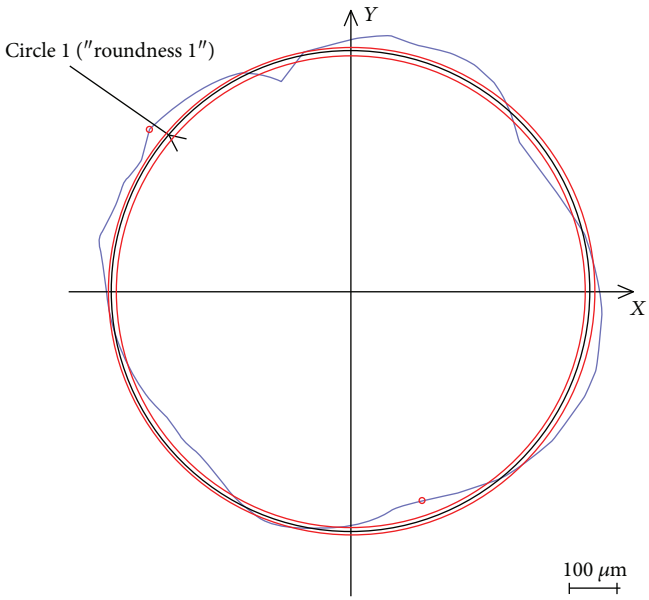

Figure 9: Circularity measurement using CMM.

The set-up for measuring delamination is shown in Figure 5. The measured data are analysed using Minitab 17.

Delamination factor with the high-speed steel (HSS) drill at the entrance of the 2 mm sample is shown in Figure 6(a). It is less at low feed rate, and its value is 1.087, while the delamination factor at the entrance for the 3 mm thickness specimen is shown in Figure 6(b). It is less at higher feed rate, and it is 1.168 at 1200 rpm. Similarly, the delamination factor at the exit side of the 2 mm sample is minimum at 0.1 mm/min feed rate with a value of 1.023 while for the 3 mm sample, it is less at higher feed rate and its value is 1.131 at 1200 rpm, as shown in Figures 6(c) and 6(d). Therefore, the delamination of the 3 mm sample at the entry and exit is minimum under the same conditions while there is a small variation with respect to the 2 mm sample. However, comparing the 2 mm and 3 mm samples, both at the entry and exit sides, the delamination factor obtained with the 2 mm sample is the minimum. Also, the error bar is included to represent the variations in the measured parameter values.

Table 2: Different control parameters and their levels.

Control parameter	Unit	Level 1	Level 2	Level 3
Thickness	mm	2	—	3
Drill bit	—	1	2	3
Feed	mm/min	0.05	0.1	0.15
Speed	rpm	800	1000	1200

The delamination factor with the titanium-coated HSS drill at the entrance of the 2 mm sample is shown in Figure 6(e). It is less at 0.1 mm/min feed rate and at 1200 rpm whose value is 1.028 while the delamination factor is minimum for the 3 mm sample at a feed rate of 0.1 mm/min and at 1000 rpm whose value is 1.031, as shown in Figure 6(f). Similarly, the delamination factor at the exit of the 2 mm sample is minimum at 0.1 mm/min feed rate and at 1200 rpm whose value is 1.037 while for the 3 mm sample, the delamination factor is minimum at 0.05 mm/min and at 1200 rpm whose value is 1.081. Therefore, delamination of the 2 mm sample at the entry and exit is minimum under the same conditions while there is a small variation with respect to the 3 mm sample. The delamination at the entry and exit is shown with an error bar in Figures 6(e)–6(h).

Table 3: ANOVA analysis for surface roughness.

Source	DF	Seq SS	Analysis of variance Contribution	Adj SS	Adj MS	*F* value	*P* value
Model	13	247.686	95.33%	247.686	19.053	50.3	0
Linear	4	159.384	61.35%	163.418	40.855	107.86	0
Drill bit	1	142.891	55%	140.711	140.711	371.47	0
Feed	1	2.901	1.12%	4.785	4.785	12.63	0.001
Speed	1	12.277	4.73%	14.827	14.827	39.14	0
Square	3	30.065	11.57%	28.381	9.46	24.97	0
Drill bit * drill bit	1	22.863	8.80%	10.112	10.112	26.69	0
Feed * feed	1	6.474	2.49%	10.199	10.199	26.92	0
2-way interaction	6	58.237	22.42%	58.237	9.706	25.62	0
Thickness * drill bit	1	44.192	17.01%	50.761	50.761	134.01	0
Thickness * feed	1	10.067	3.87%	10.476	10.476	27.66	0
Drill bit * speed	1	2.308	0.89%	2.322	2.322	6.13	0.019
Error	32	12.121	4.67%	12.121	0.379		
Total	45	259.808	100.00%				
S	*R*-sq	*R*-sq (adj)	PRESS	*R*-sq (pred)			
0.615460	95.33%	93.44%	24.3310	90.63%			

Table 4: ANOVA analysis for circularity.

Source	DF	Seq SS	Contribution	Adj SS	Adj MS	*F* value	*P* value
Model	13	0.256581	79.58%	0.256581	0.019737	9.29	0
Linear	4	0.093656	29.05%	0.127721	0.03193	15.03	0
Thickness	1	0.010347	3.21%	0.012988	0.012988	6.11	0.019
Drill bit	1	0.018212	5.65%	0.034247	0.034247	16.12	0
Feed	1	0.045643	14.16%	0.07398	0.07398	34.83	0
Speed	1	0.019454	6.03%	0.020088	0.020088	9.46	0.004
Square	3	0.137807	42.74%	0.136883	0.045628	21.48	0
Drill bit * drill bit	1	0.039647	12.30%	0.058714	0.058714	27.64	0
Speed * speed	1	0.092445	28.67%	0.093571	0.093571	44.05	0
Thickness * feed	1	0.01357	4.21%	0.011942	0.011942	5.62	0.024
Error	31	0.065849	20.42%	0.065849	0.002124		
Total	44	0.322431	100.00%				
S	*R*-sq	*R*-sq (adj)	PRESS	*R*-sq (pred)			
0.0460888	79.58%	71.01%	0.131806	59.12%			

The delamination factor with the carbide tip drill at the entrance of the 2 mm sample is shown in Figure 6(i). It is minimum at 0.05 mm/min feed rate and at 1200 rpm whose value is 1.087 while the delamination factor is minimum for the 3 mm sample at 0.05 mm/min feed rate and at 1000 rpm whose value is 1.121, as shown in Figure 6(j). Similarly, the delamination factor at the exit of the 2 mm sample is minimum at 0.1 mm/min and at 1000 rpm whose value is 1.026 as shown in Figure 6(k) while the delamination factor for the 3 mm sample is minimum at 0.5 mm/min and at 1200 rpm whose value is 1.078, as shown in Figure 6(l). Therefore, it is inferred from the graphs that the delamination factor is minimum with the 2 mm sample when compared with the 3 mm sample. The error bar is also represented in the graphs to predict the uncertainty in the measured parameter values.

Hence, it is concluded from Figures 6(a)–6(l) that the usage of the HSS drill, titanium-coated HSS drill, and carbide tip drill yields less delamination factor both at the entry and exit with the 2 mm sample than the 3 mm sample.

3.2. Surface Roughness Measurement. Surface roughness is measured using a computerized surface roughness tester with a diamond stylus of 2 μm radius, and the set-up is shown in Figure 7.

The surface roughness of the hole drilled using the HSS drill and titanium-coated HSS drill is minimal at low feed rate and high speed. Similarly, the usage of a carbide tip drill

Table 5: ANOVA analysis for delamination entry.

Source	DF	Seq SS	Analysis of variance Contribution	Adj SS	Adj MS	*F* value	*P* value
Model	13	0.03751	99.81%	0.03751	0.002885	530.76	0
Linear	4	0.021681	57.69%	0.007774	0.001944	357.52	0
Thickness	1	0.018327	48.77%	0.006198	0.006198	1140.17	0
Drill bit	1	0.000015	0.04%	0.000224	0.000224	41.22	0
Feed	1	0.003007	8.00%	0.000554	0.000554	101.93	0
Speed	1	0.000332	0.88%	0.000041	0.000041	7.61	0.016
Square	3	0.000468	1.25%	0.000359	0.00012	22.02	0
Drill bit * drill bit	1	0.000329	0.88%	0.000326	0.000326	59.93	0
Speed * speed	1	0	0.00%	0.000026	0.000026	4.78	0.048
2-way interaction	6	0.015362	40.88%	0.015362	0.00256	470.95	0
Thickness * drill bit	1	0.012946	34.45%	0.007243	0.007243	1332.37	0
Thickness * feed	1	0.000972	2.59%	0.00133	0.00133	244.62	0
Thickness * speed	1	0.000598	1.59%	0.000665	0.000665	122.39	0
Drill bit * feed	1	0.000773	2.06%	0.000477	0.000477	87.82	0
Feed * speed	1	0.00004	0.11%	0.00004	0.00004	7.36	0.018
Error	13	0.000071	0.19%	0.000071	0.000005		
Total	26	0.037581	100.00%				
S	*R*-sq	*R*-sq (adj)	PRESS	*R*-sq (pred)			
0.0023316	99.81%	99.62%	0.0002890	99.23%			

Table 6: ANOVA analysis for delamination exit.

Source	DF	Seq SS	Analysis of variance Contribution	Adj SS	Adj MS	*F* value	*P* value
Model	13	0.058171	69.36%	0.058171	0.004475	5.05	0
Linear	4	0.023373	27.87%	0.024854	0.006214	7.01	0
Drill bit	1	0.00524	6.25%	0.004373	0.004373	4.94	0.034
Feed	1	0.012731	15.18%	0.016748	0.016748	18.9	0
Square	3	0.016344	19.49%	0.01552	0.005173	5.84	0.003
Feed * feed	1	0.015351	18.30%	0.012999	0.012999	14.67	0.001
2-way interaction	6	0.018454	22.01%	0.018454	0.003076	3.47	0.01
Thickness * feed	1	0.017181	20.49%	0.017772	0.017772	20.06	0
Error	29	0.025692	30.64%	0.025692	0.000886		
Total	42	0.083863	100.00%				
S	*R*-sq	*R*-sq (adj)	PRESS	*R*-sq (pred)			
0.0297645	69.36%	55.63%	0.0577628	31.12%			

tool follows a regular pattern with the 2 mm sample, and it is disturbed in the case of 1000 rpm. At 1000 rpm, there is a peak rise at maximum feed with the 2 mm sample. But as far as surface roughness is considered, it is minimal at maximum speed and at minimum feed rate with respect to the 2 mm sample. All the graphs from Figures 8(a)–8(c) are represented with an error bar.

Surface roughness is minimum at 0.1 mm/min feed rate and at high speed with respect to the 3 mm thick specimen of the HSS drilled hole. As the thickness of the workpiece is increased, the feed rate has to be increased further, as inferred from Figure 8(d). But when the titanium-coated HSS drill is considered, the surface roughness is minimum at high feed rate and high speed conditions as shown in Figure 8(e). The surface roughness is also minimum at maximum feed and speed when the hole is drilled with the carbide tip drill tool. In Figures 8(d)–8(f), the error bar is represented to show the variations in the measured values.

Thus, it is concluded that the surface roughness is minimum at less feed rate and high speed with the 2 mm sample while the surface roughness is minimum at high feed rate and high speed with the 3 mm sample. This is because as the selected thickness is increased, the feed rate needs to be increased further, so that the surface is smooth. According to Kumar et al., the occurrence of fracture is less under less feed and at high speed. The same criteria are also applicable

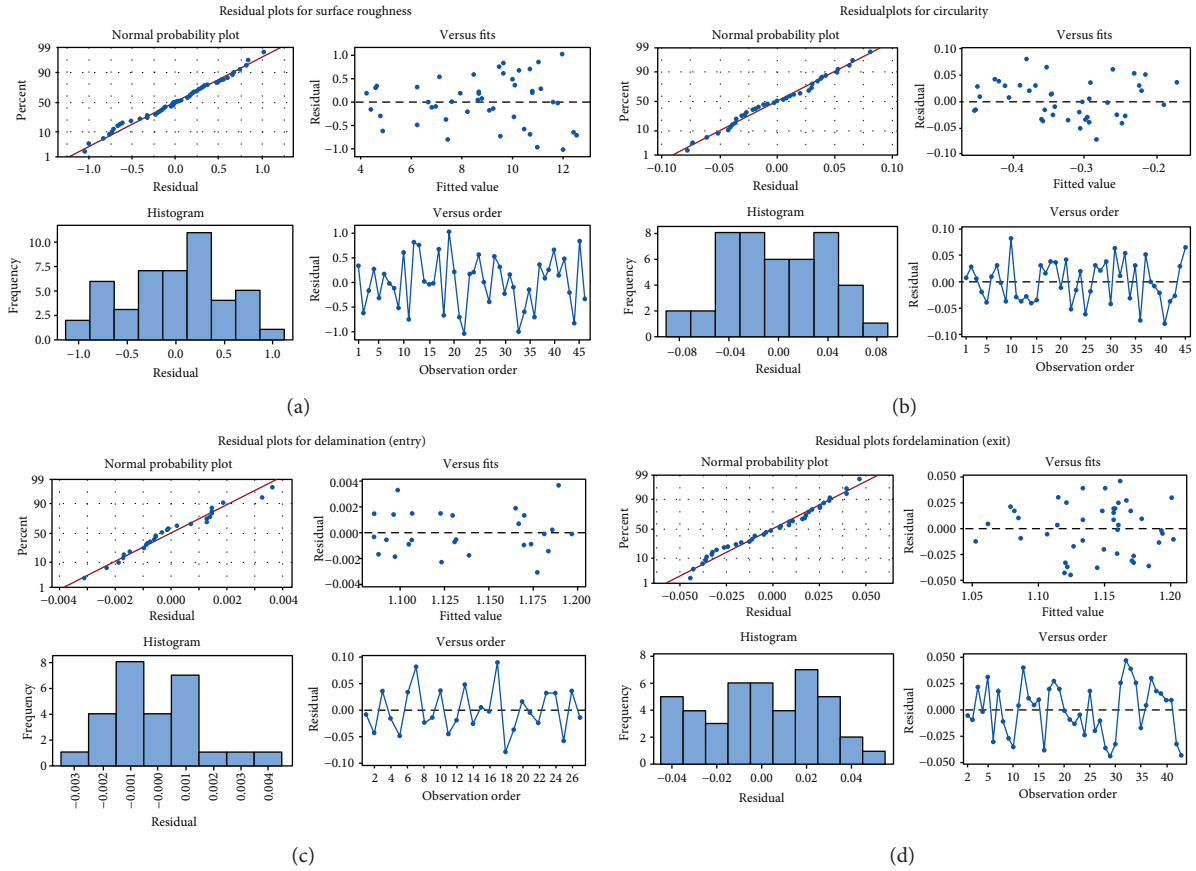

Figure 10: Residual plots: (a) surface roughness, (b) circularity, (c) delamination at entry, and (d) delamination at exit.

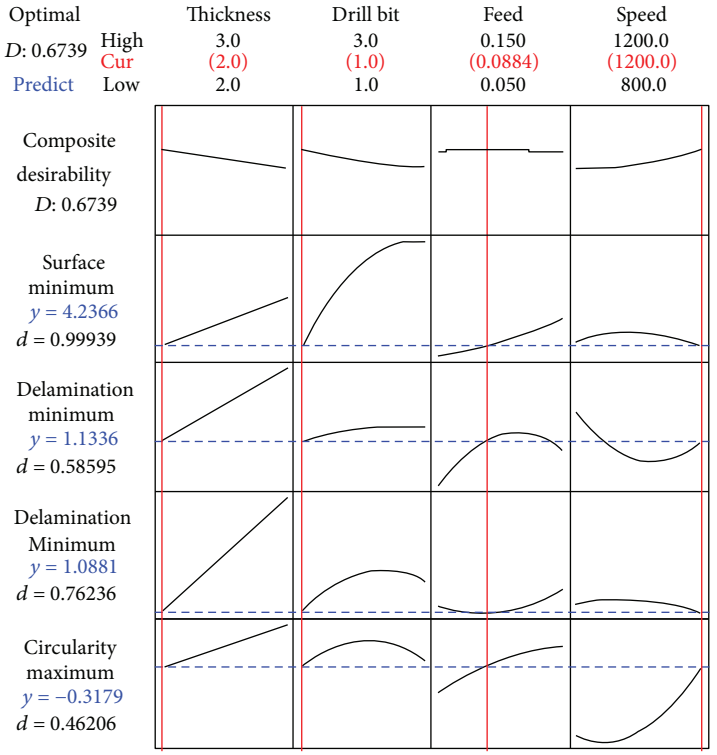

Figure 11: Optimization plot.

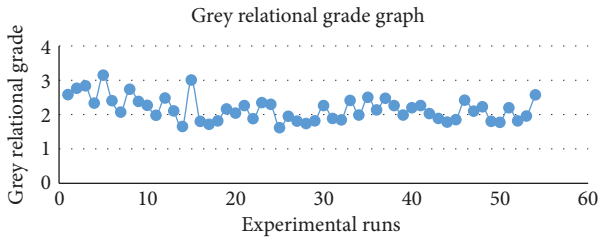

Figure 12: Grey relational grade versus experimental runs.

to the current study. Apart from this, the present work deals with different thicknesses of the specimen. Kumar et al. observed that when the thickness was minimum, the conditions were satisfied but as the thickness of the specimen was increased, the above-stated conditions differed.

3.3. Circularity Measurement of Drilled Hole. Circularity is measured using a ZEISS Contura G2 coordinate measuring machine, and one of the profiles obtained is shown in Figure 9. Figure 9 represents the profile for the 3 mm thickness specimen drilled with the HSS drill tool material under 0.15 mm/min feed rate and 1000 rpm speed. The various control parameters and their levels are represented in Table 2.

4. Results and Discussion

4.1. Surface Roughness. ANOVA technique is used for determining the most significant statistical parameter which influences the drilling operation of a biaxial noncrimp fabric composite. It also determines the percentage contribution of each control parameter during the drilling process. The results of the ANOVA analysis are shown in Tables 3–6. Analysis is carried out to a confidence level of 95% (significance level is 5%). From Table 3, it is understood that the type of drill bit, speed, feed, and thickness influenced the surface roughness values by 55%, 4.73%, 1.12%, and 0.51%, respectively. Since the P value is lower than 0.05, it is observed that the type of drill bit and speed have physical significance on surface roughness, especially the type of drill used for drilling purpose. Also, since the P value is more than 0.05, it is considered as insignificant and it is ignored.

4.2. Circularity. The most significant factor for circularity is feed rate with a contribution of 14.16% which is then followed by speed, drill bit material, and thickness of specimen. This inference is drawn on the basis of Table 4. Since the P value is more than 0.05, it is considered as insignificant and it is ignored.

4.3. Delamination at Entry. The thickness, feed, speed, and drill bit affected the delamination entry by 48.77%, 8%, 0.88%, and 0.04%, respectively. The thickness of the specimen and feed rate had physical and statistical significance on delamination entry especially the thickness of the specimen. Table 5 gives this inference about the delamination entry of the drilled hole. Since the P value is more than 0.05, it is considered as insignificant and it is ignored.

4.4. Delamination at Exit. For the delamination at exit, the most influencing factor is feed with 15.18% contribution which is then followed by drill bit, speed, and thickness. Table 6 represents these values at the exit side of the drilled hole. Since the P value is more than 0.05, it is considered as insignificant and it is ignored.

The various residual plots for surface roughness, circularity, and delamination entry and exit are shown in Figures 10(a)–10(d). It is observed from the normal probability plots of all the four parameters that most of the values are best fitted with the straight line. The regression equations for surface roughness, circularity, and delamination entry and exit are developed using response surface methodology in order to predict the output responses. The generalized form of the regression equation is shown in the following:

$$\begin{aligned} Y = {} & \beta_0 + \beta_1 X_1 + \beta_2 X_2 + \beta_3 X_3 + \beta_4 X_4 + \beta_{12} X_2^2 \\ & + \beta_{13} X_3^2 + \beta_{14} X_4^2 + \beta_{21} X_1 X_2 + \beta_{22} X_1 X_3 \\ & + \beta_{23} X_1 X_4 + \beta_{24} X_2 X_3 + \beta_{25} X_2 X_4 + \beta_{26} X_3 X_4, \end{aligned} \quad (1)$$

where β_0 is the constant of RSM; β_1, β_2, β_3, and β_4 are the coefficients of linear variables X_1, X_2, and X_3, respectively; β_{12}, β_{13}, and β_{14} are the coefficients of squares of linear variables X_1, X_2, and X_3, respectively; β_{21}, β_{22}, β_{23}, β_{24}, β_{25}, and β_{26} are the coefficients of interaction of linear variables X_1, X_2, and X_3, respectively.

$$\begin{aligned} & \text{Surface roughness} \\ & = -28.60 + 9.53X_1 + 14.87X_2 - 15.2X_3 \\ & \quad + 0.0227X_4 - 1.101{X_2}^2 + 428.6{X_3}^2 \\ & \quad - 0.000009{X_4}^2 - 2.652X_1X_2 - 24.61X_1X_3 \\ & \quad - 0.00204X_1X_4 + 1.77X_2X_3 - 0.001720X_2X_4 \\ & \quad - 0.0038X_3X_4, \end{aligned}$$

$$\begin{aligned} & \text{Circularity} \\ & = 0.981 + 0.2639X_1 + 0.4661X_2 - 0.28X_3 - 0.004437X_4 \\ & \quad - 0.0818{X_2}^2 + 10.97{X_3}^2 + 0.000003{X_4}^2 - 0.0191X_1X_2 \\ & \quad - 0.807X_1X_3 - 0.000110X_1X_4 - 0.034X_2X_3 \\ & \quad - 0.000054X_2X_4 - 0.00085X_3X_4, \end{aligned}$$

$$\begin{aligned} & \text{Delamination (entry)} \\ & = 0.5182 + 0.24153X_1 + 0.13906X_2 + 0.629X_3 \\ & \quad + 0.000216X_4 - 0.01152{X_2}^2 - 0.231{X_3}^2 \\ & \quad - 0.000000{X_4}^2 - 0.04959X_1X_2 - 0.3949X_1X_3 \\ & \quad - 0.000060X_1X_4 + 0.1882X_2X_3 + 0.000008X_2X_4 \\ & \quad + 0.000191X_3X_4, \end{aligned}$$

$$\begin{aligned} & \text{Delamination (exit)} \\ & = 1.047 + 0.0790X_1 - 0.0461X_2 + 6.08X_3 - 0.000491X_4 \\ & \quad + 0.01347{X_2}^2 - 15.65{X_3}^2 + 0.000000{X_4}^2 \\ & \quad - 0.0090X_1X_2 - 1.013X_1X_3 + 0.000051X_1X_4 \\ & \quad + 0.071X_2X_3 - 0.000005X_2X_4 - 0.000069X_3X_4, \end{aligned} \quad (2)$$

Table 7: Grey relational rank.

S. number	Circularity grey relational coefficient	Delamination entry grey relational coefficient	Delamination exit grey relational coefficient	Surface roughness grey relational coefficient	Grey relational grade	Rank
1	0.395296753	0.689373297	0.62529274	0.87487375	2.584836539	6
2	0.375931842	0.685636856	0.708222812	0.996031084	2.765822594	4
3	0.526080477	0.681940701	0.628235294	1	2.836256472	3
4	0.339097022	0.664041995	0.439868204	0.89231715	2.335324371	16
5	0.535660091	0.65374677	1	0.959617618	3.149024479	1
6	0.397075366	0.643765903	0.397913562	0.96409658	2.402851411	13
7	0.363542739	0.630922693	0.388646288	0.690251269	2.07336299	31
8	0.456662354	0.624691358	0.970909091	0.686720798	2.738983601	5
9	0.457846952	0.618581907	0.530815109	0.78087968	2.388123649	14
10	0.554160126	0.612590799	0.631205674	0.471489399	2.269445997	18
11	0.433128834	0.469387755	0.53722334	0.542447351	1.982187281	35
12	0.340405014	0.587006961	0.875409836	0.683817818	2.486639629	9
13	0.718940937	0.410048622	0.518446602	0.461875194	2.109311355	28
14	0.507913669	0.342354533	0.333333333	0.471903695	1.65550523	53
15	0.552425665	1	0.905084746	0.548317934	3.005828344	2
16	0.333333333	0.537154989	0.514450867	0.415757041	1.800696231	48
17	0.375931842	0.44	0.482820976	0.421860885	1.720613704	52
18	0.535660091	0.412724307	0.441322314	0.428560029	1.818266741	43
19	0.461437908	0.647058824	0.643373494	0.416269426	2.168139652	26
20	0.398870056	0.515274949	0.74789916	0.380522195	2.04256636	31
21	0.733887734	0.681940701	0.407633588	0.442435227	2.265897249	19
22	0.466314399	0.553610503	0.445742905	0.414694413	1.88036222	40
23	0.411901984	0.515274949	0.978021978	0.443384933	2.348583844	15
24	0.579638752	0.667546174	0.610983982	0.443055727	2.301224635	17
25	0.439601494	0.452593918	0.345407503	0.383292296	1.620895211	54
26	0.409988386	0.47645951	0.73553719	0.333333333	1.955318419	37
27	0.435265105	0.472897196	0.461139896	0.442982637	1.812284834	46
28	0.339097022	0.426644182	0.435562806	0.535470362	1.736774373	51
29	0.420738975	0.407407407	0.462738302	0.526876024	1.817760708	44
30	0.710261569	0.444639719	0.493530499	0.615050734	2.263482521	20
31	0.362051282	0.428087986	0.438423645	0.661350902	1.889913816	38
32	0.340405014	0.433962264	0.459552496	0.609556779	1.843476553	42
33	0.804100228	0.464220183	0.44278607	0.700149925	2.411256406	12
34	0.410942957	0.450980392	0.539393939	0.588283621	1.989600909	33
35	1	0.444639719	0.481081081	0.5800553	2.5057761	8
36	0.436341162	0.47467167	0.552795031	0.670432557	2.13424042	27
37	0.972451791	0.452593918	0.569296375	0.481741283	2.476083367	10
38	0.521418021	0.576309795	0.675949367	0.487717386	2.261394569	22
39	0.433128834	0.333333333	0.697127937	0.525304198	1.988894303	34
40	0.716024341	0.546436285	0.530815109	0.409018903	2.202294638	24
41	0.461437908	0.976833977	0.448739496	0.375938008	2.262949389	21
42	0.7827051	0.44	0.416536661	0.387915779	2.02715754	32
43	0.470039947	0.465930018	0.469244288	0.481650553	1.886864807	39
44	0.433128834	0.469387755	0.419152276	0.46251561	1.784184475	49
45	0.436341162	0.367198839	0.516441006	0.536417028	1.856398035	41
46	0.834515366	0.551198257	0.602708804	0.428696867	2.417119294	11
47	0.502133713	0.576309795	0.579175705	0.445666155	2.103285368	29
48	0.718940937	0.455855856	0.518446602	0.539228483	2.232471878	23

Table 7: Continued.

S. number	Circularity grey relational coefficient	Delamination entry grey relational coefficient	Delamination exit grey relational coefficient	Surface roughness grey relational coefficient	Grey relational grade	Rank
49	0.468791501	0.429541596	0.445742905	0.462312553	1.806388554	47
50	0.333333333	0.433962264	0.469244288	0.535999441	1.772539327	50
51	0.461437908	0.568539326	0.481081081	0.689985225	2.201043541	25
52	0.420738975	0.459165154	0.524557957	0.412972433	1.817434519	45
53	0.375931842	0.423785595	0.669172932	0.493630281	1.96252065	36
54	0.526080477	0.551198257	0.708222812	0.789315109	2.574816654	7

where X_1 is the thickness, X_2 is the drill bit (i.e., 1-HSS, 2-Ti-coated HSS, and 3-carbide tip drill), X_3 is the feed, and X_4 is the speed.

Figure 11 represents the optimization plot for a drilling operation. It shows that the most optimal tool is the HSS drill bit, when the drilling process is carried out on a lesser thickness specimen under a feed rate of 0.08 mm/min and high speed (1200 rpm).

4.5. Grey Relational Analysis. Grey relational analysis is an effective measure of analysing the drilling parameter relationship. In this analysis, initial preprocessing of the data is done so as to transfer the original sequence into a comparable sequence. Due to this, the experimental results are normalized to a range of zero and one. After data preprocessing, the grey relational coefficient is expressed as a ratio of ideal and actual normalized results as depicted in the following equation with different parameters:

$$\varsigma_i(k) = \frac{\Delta_{\min} + \varsigma \cdot \Delta_{\max}}{\Delta_{0i}(k) + \varsigma \cdot \Delta_{\max}}, \tag{3}$$

where $\Delta_{0i}(k)$ is the deviation sequence of the reference sequence $x_0^*(k)$ and the comparability sequence $x_i^*(k)$, namely,

$$\begin{aligned} &\Delta_{0i}(k) = \|x_0^*(k) - x_i^*(k)\|, \\ &\Delta_{\max} = \max \quad \max \|x_0^*(k) - x_i^*(k)\| \quad \forall j, \varepsilon_i, \forall k, \\ &\Delta_{\min} = \min \quad \min \|x_0^*(k) - x_i^*(k)\| \quad \forall j, \varepsilon_i, \forall k. \end{aligned} \tag{4}$$

ς is the identification coefficient and it is assumed to be equal to 0.5 usually, and the grey relational grade is given by the following equation:

$$\gamma_i = \frac{1^n}{\Sigma \zeta_i(k)}, \quad n, k = 1. \tag{5}$$

For the present study, the target values are set as minimum for surface roughness and delamination at entry and exit and maximum for circularity. Also, from the experimental design, as observed from Figure 12 and Table 7, the drilling operation parameters set for experiment number 5 gives the best optimal performance characteristics among all the 54 experiments.

5. Conclusion

From the present study, the following points are concluded:

(i) Using response surface methodology, the most optimal drilling parameters for drilling biaxial GFRP with a graphene platelet nanopowder composite are found to be with the HSS drill bit on 2 mm thickness specimen under limiting factors of high speed and low feed rate.

(ii) Using grey relational analysis, the most optimal conditions for drilling biaxial GFRP with a graphene platelet nanopowder composite is found to be with the HSS drill on 2 mm thickness specimen with low feed rate at the selected 1000 rpm speed.

Therefore, by comparing the two methods, the most optimal conditions of the drilling process are found to be the same. Thus, for minimum thickness of biaxial GFRP with the graphene platelet nanopowder composite, the HSS drill suits well and the delamination at the entry and exit is minimum with the 2 and 3 mm thickness specimens. Also, the surface roughness is minimum, and the circularity is maximum with the 2 mm thickness specimen which is drilled with the HSS drill bit.

Hence, it is concluded that for the biaxial nanocomposite, the drilling operation performed using the HSS drill bit on 2 mm thickness specimen under high speed and low feed rate yielded minimum delamination at the entry and exit, minimum surface roughness, and maximum circularity when compared to titanium-coated HSS drill and carbide tip drill tools.

Conflicts of Interest

The authors declare that there is no conflict of interest regarding the publication of this paper.

References

[1] B. A. Rezende, M. L. Silveira, L. M. G. Vieira, A. M. Abrão, P. E. de Faria, and J. C. Campos Rubio, "Investigation on the effect of drill geometry and pilot holes on thrust force and burr height when drilling an aluminium/PE sandwich material," *Materials*, vol. 9, no. 9, 2016.

[2] D. Kumar, K. K. Singh, and R. Zitoune, "Experimental investigation of delamination and surface roughness in the drilling of GFRP composite material with different drills," *Advanced Manufacturing: Polymer & Composites Science*, vol. 2, no. 2, pp. 47–56, 2016.

[3] D. Babu, K. Sivaji Babu, and B. Uma Maheswar Gowd, "Drilling uni-directional fiber-reinforced plastics manufactured by hand lay-up: influence of fibers," *American Journal of Materials Science and Technology*, vol. 1, pp. 1–10, 2012.

[4] T. J. Grilo, R. M. F. Paulo, C. R. M. Silva, and J. P. Davim, "Experimental delamination analyses of CFRPs using different drill geometries," *Composites Part B: Engineering*, vol. 45, no. 1, pp. 1344–1350, 2013.

[5] I. Asiltürk and S. Neseli, "Multi response optimisation of CNC turning parameters via Taguchi method-based response surface analysis," *Measurement*, vol. 45, no. 4, pp. 785–794, 2012.

[6] U. A. Khashaba and A. A. El-Keran, "Drilling analysis of thin woven glass-fiber reinforced epoxy composites," *Journal of Materials Processing Technology*, vol. 249, pp. 415–425, 2017.

[7] K. Debnath, I. Singh, and T. S. Srivatsan, "An innovative tool for engineering good-quality holes in composite laminates," *Materials and Manufacturing Processes*, vol. 32, no. 9, pp. 952–957, 2016.

[8] R. M. Kulkarni, H. N. Narasimha Murthy, G. B. Rudrakshi, and Sushilendra, "Effect of drilling parameters in drilling of glass fiber reinforced vinyl ester/carbon black nanocomposites," *International Journal of Scientific & Technology Research*, vol. 3, no. 7, 2014.

[9] N. S. Mohan, S. M. Kulkarni, and A. Ramachandra, "Delamination analysis in drilling process of glass fiber reinforced plastic (GFRP) composite materials," *Journal of Materials Processing Technology*, vol. 186, no. 1-3, pp. 265–271, 2007.

[10] M. Mudhukrishnan, P. Hariharan, K. Palanikumar, and B. Latha, "Tool materials influence on surface roughness and oversize in machining glass fiber reinforced polypropylene (GFR-PP) composites," *Materials and Manufacturing Processes*, vol. 32, no. 9, pp. 988–997, 2016.

[11] K. Palanikumar and J. P. Davim, "Assessment of some factors influencing tool wear on the machining of glass fibre-reinforced plastics by coated cemented carbide tools," *Journal of Materials Processing Technology*, vol. 209, no. 1, pp. 511–519, 2009.

[12] K. Palanikumar, "Modeling and analysis of delamination factor and surface roughness in drilling GFRP composites," *Materials and Manufacturing Processes*, vol. 25, no. 10, pp. 1059–1067, 2010.

[13] R. Q. Sardinas, P. Reis, and J. P. Davim, "Multi-objective optimization of cutting parameters for drilling laminate composite materials by using genetic algorithms," *Composites Science and Technology*, vol. 66, no. 15, pp. 3083–3088, 2006.

[14] V. Sridharan, T. Raja, and N. Muthukrishnan, "Study of the effect of matrix, fibre treatment and graphene on delamination by drilling jute/epoxy nanohybrid composite," *Arabian Journal for Science and Engineering*, vol. 41, no. 5, pp. 1883–1894, 2016.

[15] V. K. Vankanti and V. Ganta, "Optimization of process parameters in drilling of GFRP composite using Taguchi method," *Journal of Materials Research and Technology*, vol. 3, no. 1, pp. 35–41, 2014.